Supporting Information for

Ordered Mesoporous NiO with Thin Pore Walls and Their Enhanced Sensing Performance for Formaldehyde

Xiaoyong Lai,[a,b] Guoxin Shen,[a,b] Ping Xue,*[a,b] Bingqin Yan,[a,b] Hong Wang,[c] Peng Li [a], Weitao Xia [a] and Junzhuo Fang [a]*

[a] Key Laboratory of Energy Resource and Chemical Engineering, State Key Laboratory Cultivation Base of Natural Gas Conversion, Ningxia University, Yinchuan 750021, People's Republic of China.

[b] School of Chemistry and Chemical Engineering, Ningxia University, Yinchuan 750021, People's Republic of China

[c] Department of Materials and Chemical Engineering, Sichuan University of Science and Engineering, Key Laboratory of Material Corrosion and Protection of Sichuan Province, Zigong, 643000, People's Republic of China

Email：xylai@nxu.edu.cn; ping@nxu.edu.cn

Testing apparatus for gas sensing

The gas sensing measurement was performed in an apparatus as shown in Figure S1. Pt wires were used to connect the gas sensor films with a sourcemeter. DC voltage was fixed at 1 V and the current through the gas sensor film was recorded per a second. To introduce HCHO or not, dry air flow comes though the furnace at a constant speed of 600 sccm, along A-B-C-D-E-F-G-H route or A-B-E-F-G-H route, respectively. The formaldehyde concentration in the mixed gas was adjusted by using HCHO solution with different concentrations (0.005~1 wt %), and the exact values were obtained by analyzing the gas samples via the acetyl acetone spectrophotometric method.

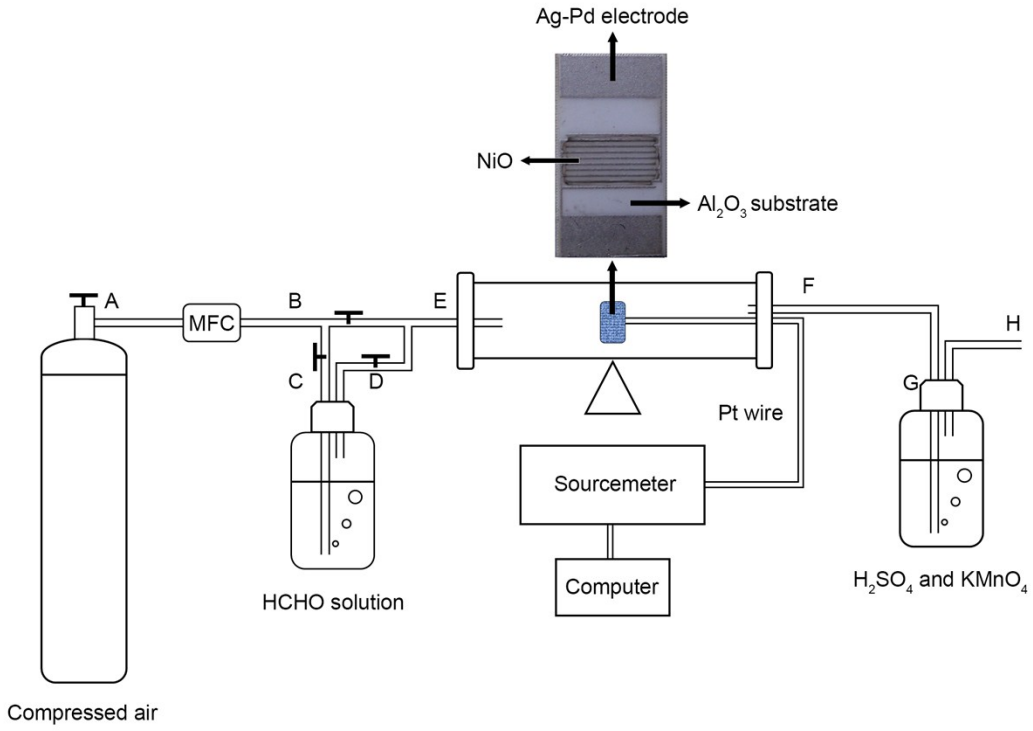

Fig. S1 Schematic diagram of the gas sensing instrument.

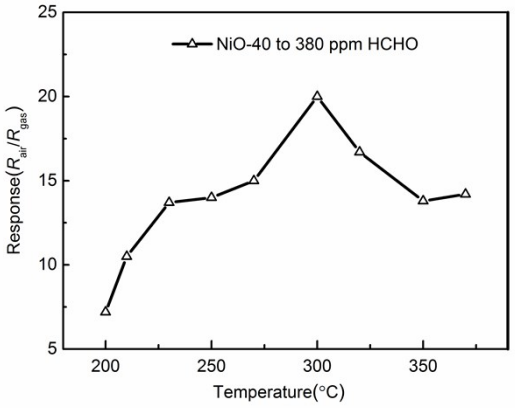

Fig. S2 Gas response versus operating temperature of NiO-40 based sensors to 380 ppm HCHO.

Preparation of NiO nanoparticles

Typically, 1.2 g of KIT-6-40 was dispersed in 10 g of ethanol solution containing 0.669 g of $Ni(NO_3)_2 \cdot 6H_2O$ precursor and then stirred at 40 °C until that ethanol was evaporated. Afterward, the resulting powder was heated in a ceramic crucible in an oven at 300 °C for 4 h, in order to decompose $Ni(NO_3)_2 \cdot 6H_2O$. The filling and heating steps were repeated once following the same conditions in

order to achieve higher loadings, except for the amounts of $Ni(NO_3)_2 \cdot 6H_2O$ were decreased to 0.627 g. Finally, the silica template was then removed at room temperature using a 2 M NaOH aqueous solution. The black NiO material was recovered by centrifugation and dried at 70 °C overnight.

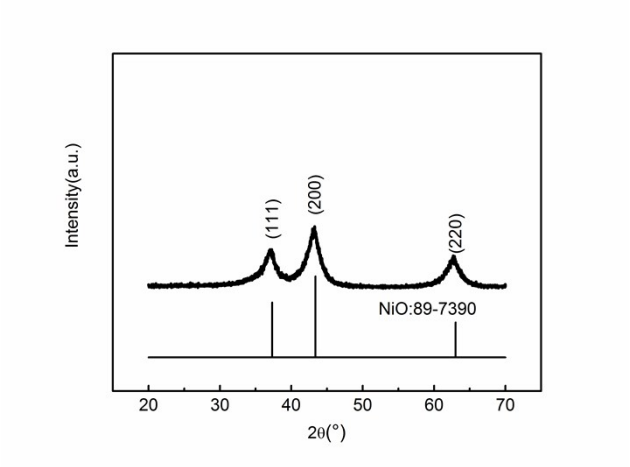

Fig. S3 XRD pattern of NiO nanoparticles

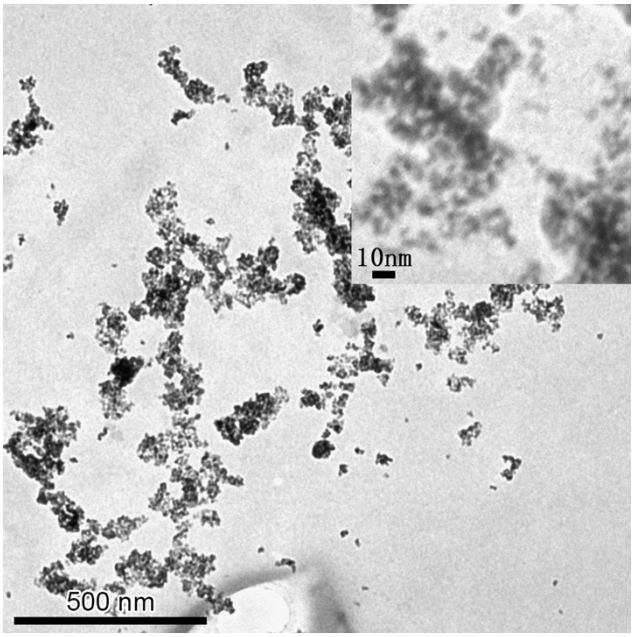

Fig. S4 TEM image of NiO nanoparticles

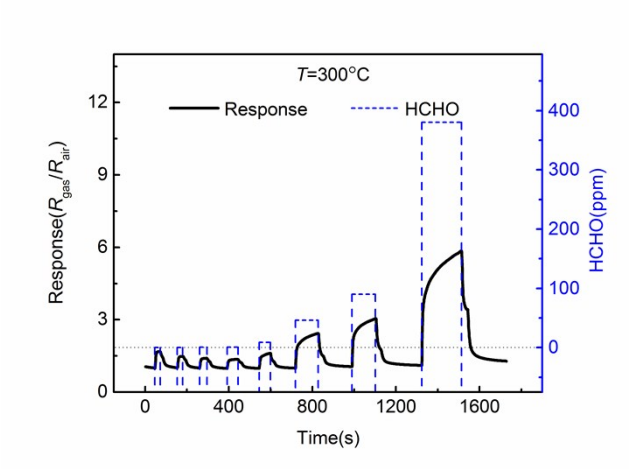

Fig. S5 Dynamic response curve of gas sensor fabricated from NiO nanoparticles, during cycling between increasing concentration of HCHO and ambient air at 300 °C.

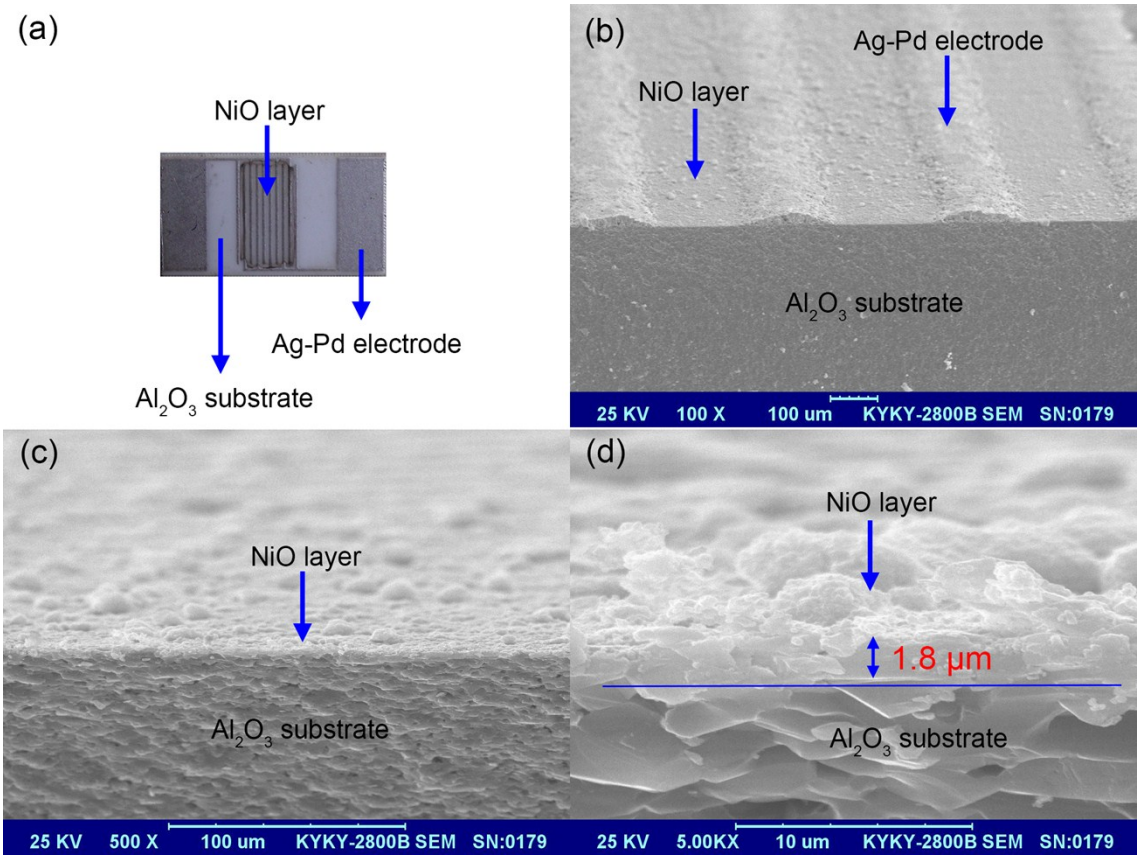

Fig. S6 a) Photograph of NiO sensor and (b, c and d) SEM images of its cross section.

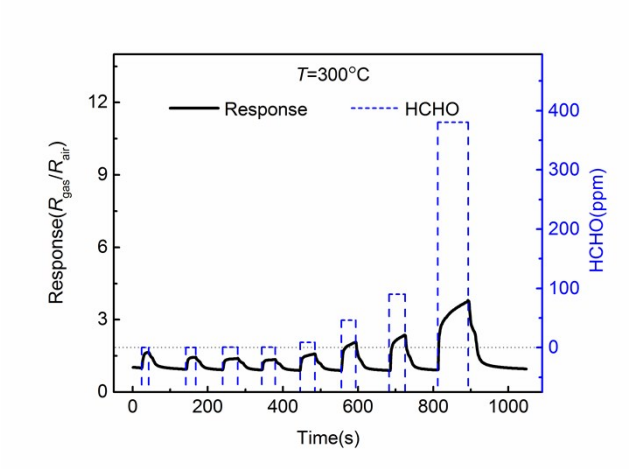

Fig. S7 Dynamic response curve of thick film based gas sensor fabricated from NiO-40, during cycling between increasing concentration of HCHO and ambient air at 300 °C.

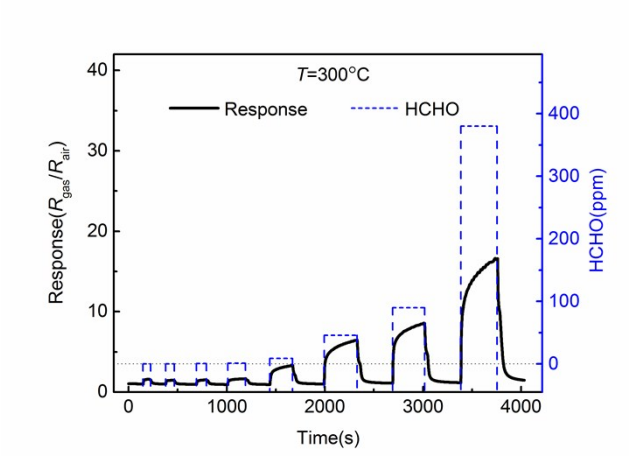

Fig. S8 Dynamic response curve of gas sensor fabricated from NiO-40 after half year, during cycling between increasing concentration of HCHO and ambient air at 300 °C.

Table S1 Comparison of the response of our sample and those reported in previous literatures, towards HCHO.

Product	Response	HCHO Concentration	Literature
Mesoporous nickel oxide NiO-40	10.2	90 ppm	This work
	7.0	46 ppm	
	3.7	9 ppm	
	2.0	1 ppm	
Au-loaded NiO hollow microsphere	2.5	50 ppm	Reference71
NiO hollow microsphere	1.3	100 ppm	Reference 72
NiO multilayer nanostructure	1.7	100 ppm	Reference 73
NiO porous nanosheets	2.3	10 ppm	Reference 74
NiO sputtered thin films	2.2	5 ppm	Reference 75